The 13-kD FK506 Binding Protein, FKBP13, Interacts with a Novel Homologue of the Erythrocyte Membrane Cytoskeletal Protein 4.1

Loren D. Walensky,*‡ Philippe Gascard,‖ Michael E. Fields,* Seth Blackshaw,* John G. Conboy,‖ Narla Mohandas,‖ and Solomon H. Snyder*‡§

*Department of Neuroscience, ‡Department of Pharmacology and Molecular Sciences, and §Department of Psychiatry and Behavioral Sciences, The Johns Hopkins University School of Medicine, Baltimore, Maryland, 21205; and ‖Life Sciences Division, Lawrence Berkeley National Laboratory, University of California, Berkeley, CA 94720

Abstract. We have identified a novel generally expressed homologue of the erythrocyte membrane cytoskeletal protein 4.1, named 4.1G, based on the interaction of its COOH-terminal domain (CTD) with the immunophilin FKBP13. The 129-amino acid peptide, designated 4.1G–CTD, is the first known physiologic binding target of FKBP13. FKBP13 is a 13-kD protein originally identified by its high affinity binding to the immunosuppressant drugs FK506 and rapamycin (Jin, Y., M.W. Albers, W.S. Lane, B.E. Bierer, and S.J. Burakoff. 1991. *Proc. Natl. Acad. Sci. USA*. 88:6677–6681); it is a membrane-associated protein thought to function as an ER chaperone (Bush, K.T., B.A. Henrickson, and S.K. Nigam. 1994. *Biochem. J.* [*Tokyo*]. 303:705–708). We report the specific association of FKBP13 with 4.1G–CTD based on yeast two-hybrid, in vitro binding and coimmunoprecipitation experiments. The histidyl-proline moiety of 4.1G–CTD is required for FKBP13 binding, as indicated by yeast experiments with truncated and mutated 4.1G–CTD constructs. In situ hybridization studies reveal cellular colocalizations for FKBP13 and 4.1G–CTD throughout the body during development, supporting a physiologic role for the interaction. Interestingly, FKBP13 cofractionates with the red blood cell homologue of 4.1 (4.1R) in ghosts, inside-out vesicles, and Triton shell preparations. The identification of FKBP13 in erythrocytes, which lack ER, suggests that FKBP13 may additionally function as a component of membrane cytoskeletal scaffolds.

THE immunophilins comprise two classes of protein receptors for the immunosuppressive drugs cyclosporin A, FK506, and rapamycin (28). Whereas cyclosporin A interacts with a family of proteins designated cyclophilins (31), FK506 and rapamycin bind to a growing family of FK506 binding proteins (FKBPs).[1] A common feature of immunophilins is their peptidyl–prolyl isomerase activity (33). FKBP12 was the first member of the FKBP family to be characterized (32). In the presence of FK506, FKBP12 binds to calcineurin and inhibits its phosphatase activity, ultimately leading to T-cell immunosupression (26, 42, 43). FKBP12 associates physiologically with two intracellular calcium channels, the ryanodine receptor (36) and the inositol 1,4,5-trisphosphate (IP$_3$) receptor (11), and regulates their ability to flux calcium. FKBP12 also interacts with type I TGFβ receptors and can inhibit the signaling pathways of TGFβ ligands (57, 58).

FKBP13 was the second member of the FKBP family to be cloned and shares 43% amino acid identity with FKBP12 (37). Whereas FKBP12 is cytosolic, FKBP13 is a membrane-associated protein, possessing an NH$_2$-terminal signal sequence and COOH-terminal RTEL motif, which are believed to play roles in protein targeting and ER retention, respectively (37). FKBP13 has been identified in rough microsomal subcellular fractions and is enriched in samples containing ER luminal proteins (46). Expression of FKBP13 is upregulated in response to heat shock

1. *Abbreviations used in this paper*: 4.1G, general protein 4.1; 4.1R, red blood cell protein 4.1; aa, amino acid(s); ala, alanine; arg, arginine; β-gal, β-galactosidase; CTD, COOH-terminal domain; EST, expressed sequence tag; FKBP, FK506 binding protein; GAL4(DB), GAL4 DNA–binding domain; GAL4(TA), GAL4 transactivating domain; gln, glutamine; HA, hemagglutinin; his, histidine; h,m,r4.1G, human, mouse, rat 4.1G; h,m,r4.1R, human, mouse, rat 4.1R; ile, isoleucine; IOV, inside-out vesicle; IP$_3$, inositol 1,4,5-trisphosphate; leu, leucine; MBD, membrane-binding domain; PEG, polyethylene glycol; pro, proline; PVDF, polyvinylene difluoride; RBC, red blood cell; RT, reverse transcription; SABD, spectrin actin-binding domain; ser, serine; trp, tryptophan; val, valine.

and the accumulation of unfolded proteins in the ER (8, 48). Taken together, these data suggested that FKBP13 may function as an ER molecular chaperone, which binds to and catalyzes the folding and/or assembly of proteins in the ER.

To further elucidate the physiologic role(s) of FKBP13, we sought to identify potential FKBP13 binding targets using the yeast two-hybrid method. We report that FKBP13 associates with the COOH-terminal domain (CTD) of a novel homologue of the red blood cell (RBC) protein 4.1 (4.1R). We have designated the new gene product 4.1G because of its general, widespread distribution compared to 4.1R, which is enriched in hematopoietic tissues and discrete neuronal populations (Walensky, L.D., Z.T. Shi, S. Blackshaw, A.C. DeVries, G.E. Demas, P. Gascard, R.J. Nelson, J.G. Conboy, E.M. Rubin, S.H. Snyder, and N. Mohandas. 1997. *Mol. Biol. Cell.* (*Suppl.*) 8:275a). 4.1R is a critical structural component of the erythrocyte membrane cytoskeleton (15). The 135- and 80-kD isoforms of 4.1R are generated by the use of alternate start codons in the coding sequence; many additional isoforms are produced by complex alternative exon splicing (16, 17, 35). The spectrin–actin binding domain (SABD) of 4.1R potentiates the interactions of spectrin tetramers with F-actin in the RBC cytoskeleton (20). 4.1R also provides a linkage between the cytoskeletal scaffold and the plasma membrane through interactions of its membrane-binding domain (MBD) with band 3 and glycophorin C (2, 49). The role of the CTD of 4.1R is unknown. 4.1G is the closest homologue to 4.1R within the 4.1 superfamily whose members contain homologous MBDs. In addition to alternative splicing of 4.1R (4, 17), 4.1G contributes to the protein 4.1 diversity observed by immunologic methods in a wide range of tissues (19, 24, 30, 54).

Materials and Methods

FKBP13 Yeast Two-hybrid Screen

Two-hybrid screening was conducted using the Y190 yeast strain containing the HIS3 and β-galactosidase (β-gal) reporter genes and the pPC86 and pPC97 expression vectors (12). The cDNA encoding rat FKBP13 was subcloned into the pPC97 vector (encoding the GAL4 DNA–binding domain [GAL4 {DB}]) and then used as bait to screen a rat hippocampal library (41) constructed in the pPC86 vector, which contains the GAL4 transcriptional activation domain (GAL4[TA]) cDNA. The FKBP13 clone was transformed into yeast using the lithium acetate/polyethylene glycol (PEG) method (3). Yeast expressing the GAL4 (BD)–FKBP13 fusion were subsequently transformed with the rat hippocampal library using a variation of the lithium acetate/PEG method. Yeast were grown to $OD_{600} = 1.0$, pelleted, and then washed with sterile water. After incubation in 100 mM lithium acetate, 10 mM Tris, pH 7.5, 1 mM EDTA, 1 M sorbital (buffer A) at 30°C for 30 min, the yeast were pelleted and resuspended in 2.5 mL of buffer A and then 50 μg of library and 800 μg of carrier DNA were added to a final volume of 3.0 mL buffer A. After adding 24 mL of 100 mM lithium acetate, 10 mM Tris, pH 7.5, 1 mM EDTA, 40% PEG, the yeast were incubated for 30 min at 30°C and then heat shocked for 15 min at 42°C. 100 mL of media lacking leucine (leu), tryptophan (trp), and histidine (his) was added and then the yeast were incubated for 3 h at 30°C. The yeast were pelleted, resuspended in leu⁻trp⁻his⁻ media, and then plated on leu⁻trp⁻his⁻ plates containing 50 mM 3-aminotriazole and then incubated at 30°C. The resulting colonies were streaked onto leu⁻trp⁻his⁻ plates and then tested for β-gal activity as previously described (12). The plasmid was isolated from a colony displaying β-gal activity using glass beads (3), transformed into bacteria by electroporation, and then DNA sequenced. The plasmid encoded a 129-amino acid (aa) peptide with sequence homology to the CTD of 4.1R, as determined by

searching the National Center for Biotechnology Information sequence databases (Bethesda, MD) using the BLAST network service. The sequence alignment was generated using the Geneworks program (Oxford Molecular Group, Oxford, UK).

pPC97 containing the FKBP13 target (rat 4.1G[r4.1G]–CTD), fos, FKBP12, and pPC86 containing jun, were generated for control experiments. Vectors lacking inserts were likewise used to assess nonspecific lacZ activation by r4.1G–CTD with the GAL4 binding or activating domains alone. Y190 yeast were cotransformed with pPC97 and pPC86 constructs using the lithium acetate/PEG method, restreaked onto leu⁻trp⁻ plates, and then assessed for β-gal activity using the nitrocellulose lift assay. To determine whether the interaction between FKBP13 and its target was sensitive to FK506, the double transformants were plated on leu⁻trp⁻ plates containing vehicle (ethanol), 1-, 10-, and 50-μM FK506. Fos–jun double transformants were used as a positive control in these experiments.

Southern Analysis of 4.1G–CTD

Genomic DNA prepared from rat tail was digested with 20 U BamH1/μg DNA. The DNA was subjected to 0.7% agarose gel electrophoresis and then stained with ethidium bromide. The gel was then depurinated with 0.2 N HCl for 10 min, denatured with 0.5 N NaOH/1.5 M NaCl for 45 min, neutralized with 1 M Tris-HCl, pH 7.5, 1.5 M NaCl for 45 min and subsequently transferred and cross-linked to Hybond nylon membrane (Amersham Corp., Arlington Heights, IL). ^{32}P-labeled probes corresponding to r4.1G–CTD and the human 4.1R(h4.1R)–CTD were generated using the Multiprime kit (Amersham Corp.) according to the manufacturer's protocol. After prehybridizing for 4 h at 65°C in nylon wash buffer (14% SDS, 128 mM $Na_2HPO_4 \cdot 7H_2O$, 14 mM $Na_4EDTA \cdot 4H_2O$, 0.18% H_3PO_4, 0.2% Triton X-100), the blots were incubated overnight at 65°C with 5.0×10^6 cpm/mL probe in 0.75× wash buffer. The membranes were subsequently washed at 65°C in 0.5× wash buffer for 2 min, 0.3× wash buffer for 30 min, and 0.2× wash buffer for 20 min and then exposed to film for 2 d at −70°C.

Identification of the Mouse 4.1G cDNA

To identify the full-length cDNA containing the 387-bp 4.1G COOH-terminal sequence obtained from the yeast screen, degenerate primers were designed against 5′ 4.1R sequences conserved across species and 3′ r4.1G sequence and used in reverse transcriptase (RT)-PCR experiments using mouse brain cDNA as template. PCR was conducted with high-fidelity pfu polymerase (Stratagene, La Jolla, CA). The degenerate primers made against the CVEEHHT (5′-TGTGT[A/G]GA[A/G]CATCACACGTT) motif of the 4.1R MBD and the QHPDM (3′-CAT-[A/G]TC[T/A]GG[G/A]TGCTG) motif of the r4.1G CTD yielded a product of 965 bp. To obtain 5′ mouse 4.1G (m4.1G) sequence, the dbest database was searched using human 4.1G (h4.1G) as the query sequence (47). Mouse expressed sequence tag (EST) clone with EMBL/GenBank/DDBJ accession number AA218250 was identified and sequenced; the 3′ end of the 1652-bp clone contained the CVEEHHTFYRLVSPEQPPKTKFLTLGSK motif that overlapped with the 5′ end of the original PCR product. Sequencing of additional mouse EST clones (Genome Systems Inc., St. Louis, MO) identified exact match sequence to the PCR product and EST clone AA218250. A full-length cDNA was assembled using the following sequence data: AA218250 (bp 1–1521), W83204 (1030–1533), W17544 (1162–1528), PCR product (1441–2907), AA220495 (1807–2173), AA030412 (2554–2964), and AA009193 (2575–2964). To confirm the full-length m4.1G sequence, two pairs of nondegenerate primers were used in PCR experiments to identify overlapping products that covered the full-length cDNA. The primers were as follows: (Pair 1) 5′-MTTEVG: ATGACTACTGAAGTTGGC and 3′-RVTPLP: AGGCAGAGGTGTGACCCG; (Pair 2) 5′-CVEHHT: TGT-GTGGAACATCACACT and 3′-AEEGEE: GCGGAGGAAGGAGA-AGAA). Primers to the extreme 5′ and 3′ sequence preferentially generated shorter PCR products that represented 4.1G splice forms, and for this reason the above PCR strategy was used instead. Products of 1977 and 1523 bp were generated (in addition to smaller products determined to be splice forms) from primer pairs 1 and 2, respectively, using both mouse brain cDNA and a mouse brain cDNA library (Stratagene) as templates. All EST clones and PCR products were double-strand sequenced using the fluorescent terminator method of cycle sequencing on an automated DNA sequencer (model 373a; Applied Biosystems, Inc., Foster City, CA) at the DNA Analysis Facility of the Johns Hopkins University (45, 55). Oligonucleotides used for sequencing were generated by a synthesizer

(model 394; Applied Biosystems, Inc.) following the manufacturer's protocols. DNA sequence data was analyzed using Sequencher software from Gene Codes (Ann Arbor, MI). The m4.1G and m4.1R sequence alignment was generated using the Geneworks program (Oxford Molecular Group, Oxford, UK).

In Vitro Binding Assays

T7 his-tagged fusion proteins of r4.1G–CTD, FKBP13, and FKBP12 were generated by subcloning the corresponding cDNAs into the pet28 expression vector (Novagen, Inc., Milwaukee, WI). The corresponding GST fusion proteins of r4.1G–CTD and FKBP13 were produced by subcloning into the PGEX-4T2 expression vector (Pharmacia Biotech. Inc., Piscataway, NJ). To produce soluble FKBP13 fusion protein in the bacterial lysate, the NH$_2$-terminal signal sequence of FKBP13 was omitted in each case. Pet28 and GST expression plasmids were transformed into *Escherichia coli* BL21 (DE3) competent cells (Novagen, Inc.) and bacterial lysates containing the fusion proteins were isolated according to the manufacturer's protocol. 30 µL of a 50% slurry of glutathione-agarose (Sigma Chemical Co., St. Louis, MO) equilibrated in 50 mM Hepes, pH 7.4, 100 mM NaCl, 0.1% Tx-100 (buffer B) was added to each Eppendorf tube (Eppendorf Scientific, Inc., Hamburg, Germany) containing the GST protein extract diluted in the same buffer up to 500 µL. After rotating the tubes for 20 min at room temperature, the glutathione beads were washed three times in 1 mL of buffer B and then resuspended in 480 µL of the same buffer. 20 µL of the T7 his fusion protein lysate was added and the tubes were rotated for 1 h at 4°C. In FK506 inhibition experiments, the T7 his–FKBP13 extract was preincubated with 50 µM FK506 for 15 min at room temperature and control T7 his–FKBP13 extract was incubated with vehicle (1% ethanol). The beads were then washed five times with 500 µL of 50 mM Hepes, pH 7.4, 400 mM NaCl, 0.1% Triton X-100 (Tx-100), resuspended in PBS/protein load buffer, and subjected to electrophoresis using 18% tris-glycine minigels (Novex, San Diego, CA). Proteins were wet transferred to polyvinylene difluoride (PVDF) membrane (Millipore Corp., Waters Chromatography, Bedford, MA), blocked for 2 h in 5% nonfat dry milk, and incubated with 1:5,000 rabbit anti-GST (Santa Cruz Biotechnology, Inc., Santa Cruz, CA) and 1:5,000 mouse anti-T7 (Novagen Inc.) primary antibodies for 1 h at room temperature. Blots were washed in 5% milk one time for 15 min and two times for 5 min, followed by a 1-h incubation at room temperature in 1:5,000 anti-rabbit and 1:5,000 anti-mouse secondary antibodies (Boehringer Mannheim Biochemicals, Indianapolis, IN). After washing in 5% milk one time for 15 min and 0.1% Tween (Sigma Chemical Co.)/PBS two times for 10 min, Western blots were developed by chemiluminescence using the Renaissance kit (NEN Dupont, Boston, MA) according to the manufacturer's protocol.

HEK 293 Cell Transfection and Coimmunoprecipitation

HEK 293 cells were transfected by the calcium phosphate precipitation method (52) with 9 µg of the NH$_2$-terminal c-*myc*–r4.1G–CTD vector alone or in combination with 1 µg of the COOH-terminal hemagglutinin (HA)–FKBP13 vector. The inserts were generated by PCR using primers containing Sal1 and Not1 sites for subcloning into a cytomegalovirus promoter-driven mammalian expression vector. After 24 h, the cells were washed with 3 mL PBS and then treated with 1 mL of lysis buffer (50 mM Trizma [Sigma Chemical Co.], pH 7.4, 40 mM NaCl, 0.5% CHAPS, or 0.5% Triton X-100, 4 µg/mL leupeptin, 2 µg/mL antipain, 2 µg/mL chymotrypsin, 2 µg/mL pepstatin, 1 mM PMSF) on ice for 10 min. Supernatants were isolated after centrifugation at 14,000 *g* for 10 min at 4°C. 1 µL of mouse monoclonal anti–HA antibody (BAbCO, Berkeley, CA) was added to 400 µL of supernatant and incubated from 2 h to overnight at 4°C. 40 µL of a 50% protein A–agarose slurry (Oncogene Science Inc., Cambridge, MA) was then added followed by a 1-h incubation at 4°C. The beads were then washed on ice with 50 mM Trizma, pH 7.4, 150 mM NaCl, 0.5% CHAPS, or 0.5% Tx-100. The contents were eluted in SDS-PAGE sample buffer, electrophoresed on 18% tris-glycine minigels (Novex), and immunoblotted with affinity-purified mouse monoclonal anti–c-*myc* antibody (Oncogene Science Inc.). 20 µL of cell lysates were likewise electrophoresed on 18% gels and immunoblotted with a mixture of the anti–c-*myc* antibody and the mouse monoclonal anti-HA antiserum (BAbCO).

Mutational Analysis

Deletion mutants of r4.1G–CTD were generated by PCR and subcloned

into pPC86 using Sal1 and Not1 restriction sites. Pro(108) to alanine (ala), his(107) to leu, and his(107) to arginine (arg) point mutations were constructed by the overlap extension method (34). GAL4(TA)–r4.1G–CTD constructs were cotransformed into Y190 yeast with GAL4-(DB)–FKBP13 as described above. Double transformants were restreaked onto leu⁻trp⁻ plates and assayed for β-gal activity using the nitrocellulose lift filter assay.

FKBP Antibodies

cDNAs encoding FKBP13 (without the NH$_2$-terminal signal sequence) and FKBP12 were subcloned into the pet22b expression vector (Novagen Inc.). *E. coli* BL21 (DE3) bacteria (Novagen Inc.) were transformed and the fusion proteins expressed and purified over nickel columns (Novagen Inc.) according to the manufacturer's protocol. New Zealand white rabbits were immunized with the FKBP antigens according to established protocols (Hazleton Labs, Denver, PA) except that alternating injections consisted of FKBP/45-nm colloidal gold (E.Y. Laboratories, Inc., San Mateo, CA) conjugates to increase the immunologic response (50). Production bleeds were affinity purified by first passing the serum over affigel-10 (Bio-Rad Laboratories, Hercules, CA) columns containing pet 22b fusion protein lacking the FKBP inserts. Flowthroughs were then passed over the respective FKBP affigel-10 columns. After extensive washing with 10 mM Tris, pH 7.5, and 10 mM Tris, pH 7.5, 500 mM NaCl, the antibodies were eluted with 100 mM glycine, pH 2.5, and 100 mM triethylamine, pH 11.5, and dialyzed against PBS and PBS/40% glycerol for storage. Antibody specificity was evaluated by Western analysis using brain extracts prepared by homogenizing whole rat brain in ice-cold lysis buffer C containing 10 mM Tris, pH 8.0, 150 mM NaCl, 0.1% SDS, 1% NP-40, 1% sodium deoxycholate, 1 mM EDTA, protease inhibitors (as above), followed by centrifugation at 39,000 *g* for 20 min at 4°C. The extract was protein assayed using DC reagents (Bio-Rad Laboratories) and 5 µg of protein per lane was electrophoresed on an 18% tris-glycine polyacrylamide gel. A silver-stained lane containing FKBPs purified from whole brain on an FK506 column (see below) served as FKBP molecular weight markers. Western analysis was conducted as described above. Anti-FKBP12 and -FKBP13 antibodies were diluted 1:250 in 3% BSA/PBS. Blocking experiments were conducted by preadsorbing the antibodies with purified FKBP fusion protein overnight at 4°C.

FK506 Column Synthesis

FK506 was chemically derivatized and coupled to affigel-10 (Bio-Rad Laboratories) as previously described (25). FK506 was a gift of S. Hasimoto (Exploratory Research Laboratories, Fujisawa Pharmaceutical Co., Tsukuba, Japan).

Red Blood Cell Preparations

Sprague Dawley rat RBCs and ghosts were isolated according to established procedures (5). The cytosol was obtained by hypotonic lysis of purified RBCs and subsequently treated with chloroform and water extraction to remove the hemoglobin (38). Ghosts were solubilized in lysis buffer C (see above). The RBC fractions were protein assayed using DC reagents (Bio-Rad Laboratories), and 20 µg of each were analyzed by gel electrophoresis on 18% tris-glycine polyacrylamide gels, wet transferred to PVDF, and then probed with anti-FKBP12 and -FKBP13 antibodies as described above. 10 µg of brain extract (prepared as above) served as positive controls. The solubilized ghosts were also incubated with the FK506 matrix to concentrate ghost-associated FKBP. 200 µL of solubilized rat ghosts were incubated with 30 µL of a 50% FK506 matrix slurry preequilibrated with 50 mM Trizma, pH 7.4, 100 mM NaCl, 0.1% Tx-100 and brought to a final volume of 500 µL with this buffer. Specific binding to the matrix was assessed by adding 100 µM of free FK506 to control samples. The final vehicle (ethanol) concentration in each tube was 2.0%. After rotating the samples for 2 h at 4°C, the matrix was washed by incubating three times for 20 min with 1 mL of 0.05% Tween/PBS at 4°C. The pelleted matrix was resuspended in PBS/protein load buffer, electrophoresed on 18% tris-glycine gels, wet transferred to PVDF, and subjected to anti-FKBP Western analysis.

For fractionation experiments, RBCs were purified based on established methods (6). Briefly, rat RBCs were withdrawn on EDTA, resuspended with PBS, and pelleted (770 *g*, 10 min) three times to remove the buffy coat. To remove remaining leukocytes and platelets, the washed blood was resuspended at a hematocrit of 10% in ice-cold PBS and loaded

onto a column of equal volume containing 3:1 alpha-cellulose (Sigma Chemical Co.) to Sigmacell cellulose type 50 (Sigma Chemical Co.) pre-equilibrated in PBS. Blood was collected by gravity flow and washed with PBS three times. Ghosts were obtained by lysing purified RBCs in 30 vol of hypotonic lysis buffer (ice-cold 10 mM sodium phosphate, pH 7.4) for 5 min on ice. After centrifugation for 10 min at 4°C (SS34 rotor, 16,000 rpm; Sorvall Instruments Division, Dupont Co., Newton, CT), the pelleted ghosts were washed in 30 vol of hypotonic lysis buffer until they became white. Inside-out vesicles (IOVs) and stripped IOVs were prepared as previously described (29). Briefly, ghosts were incubated in 30 vol 0.1 mM EGTA, pH 8.5, at 37°C for 30 min. The resulting IOVs were centrifuged for 20 min at 4°C, washed once with hypotonic lysis buffer, and then resuspended in the same buffer. Stripped IOVs were prepared by incubating IOVs in 30 vol of 0.1 mM EGTA, pH 11, at 25°C for 20 min, followed by centrifugation and washing as described for IOVs. Triton shells were generated by incubating ghosts in 20 vol of 625 mM NaCl/6.25 mM sodium phosphate, pH 7.0, 0.625 mM EGTA, 0.625 mM DTT, 2.0% Tx-100 for 30 min at 4°C (23). The resulting Triton shells were centrifuged and washed as described for IOVs. 20 μg of each fraction was electrophoresed on both 12 and 18% tris-glycine gels and then subjected to Western analysis using the FKBP13 antibody and anti 24-1, an affinity-purified anti-4.1R peptide antibody raised against the TKDVPIVHTETKTITYEAAQ motif of the CTD (18).

In Situ Hybridization

In situ hybridization using digoxigenin-labeled probes was conducted using FKBP13 and r4.1G–CTD coding sequence. Frozen 20-mm cryostat sections of 18-d-old rat embryos and 4-d-old mouse newborns were cut onto Superfrost Plus slides (Fisher Scientific Co., Pittsburgh, PA), allowed to air dry for 1–3 h, and then postfixed for 5 min in 4% paraformaldehyde/PBS. The slides were washed three times for 3 min in TBS, treated for 10 min in 0.25% acetic anhydride, 0.1 M triethanolamine, pH 8.0, washed three times for 3 min in TBS, and then prehybridized for 2 h at room temperature in hybridization buffer (50% formamide, 5× SSC, 5× Denhardt's solution, 500 mg/ml sonicated herring sperm DNA, 250 mg/ml yeast tRNA). The tissue was incubated with 0.1 mL of buffer D containing 40 ng of cRNA probe under a siliconized coverslip at 65°C overnight. After removal of the coverslips in 5× SSC at 65°C, sections were washed as follows: two times for 1 h in 0.2× SSC, one time for 5 min in 0.2× SSC,

and one time for 5 min in TBS. After a 1-h block at room temperature in 4% normal goat serum (NGS)/TBS, the slides were incubated overnight at 4°C in 1:5,000 dilution of anti-digoxigenin Fab fragment (Boehringer Mannheim Corp.) in 4% NGS/TBS. Sections were then washed three times for 5 min in TBS and one time for 5 min in buffer D (0.1 M Tris-Cl, pH 9.5, 0.1 M NaCl, 50 mM MgCl₂). The color signal was developed in buffer D containing 3.375 mg/ml nitro blue tetrazolium (Boehringer Mannheim Corp.), 3.5 mg/ml 5-bromo-4-chloro-3-indolyl phosphate (Boehringer Mannheim Corp.), and 0.24 mg/ml levamisole. The color reaction was carried out in the dark for 24–72 h at room temperature and terminated with a TE wash. The developed slides were coverslipped with Aquapolymount (Polysciences, Inc., Warington, PA). Control sections were hybridized with identical quantities of sense cRNA and no signal was observed. The in situ hybridization protocol has been used to distinguish the localizations of transcripts sharing as much as 85–90% nucleic acid identity (7, 56).

Results

Identification of a Novel 4.1 Homologue Whose CTD Interacts with FKBP13

Using the yeast two-hybrid method, we screened 2,000,000 rat hippocampal cDNA library transformants with FKBP13 as bait. Whereas 27 colonies were his positive, a single colony was both his and β-gal positive (Fig. 1 A). The deduced aa sequence of the plasmid derived from the β-gal positive colony is 129 aa in length and is 71% identical to the corresponding portion of the 4.1R–CTD encoded by exons 18–21 of the 4.1R gene (14, 35) (Fig. 1 B). No β-gal activity was observed in control experiments in which yeast were doubly transformed with combinations of FKBP13 or 4.1G–CTD and the GAL4(BD) alone, the GAL4(TA) alone, and fos and jun constructs (Fig. 1 C). Despite the robust interaction of FKBP13 with 4.1G–CTD by β-gal filter assay, no activity was observed in parallel
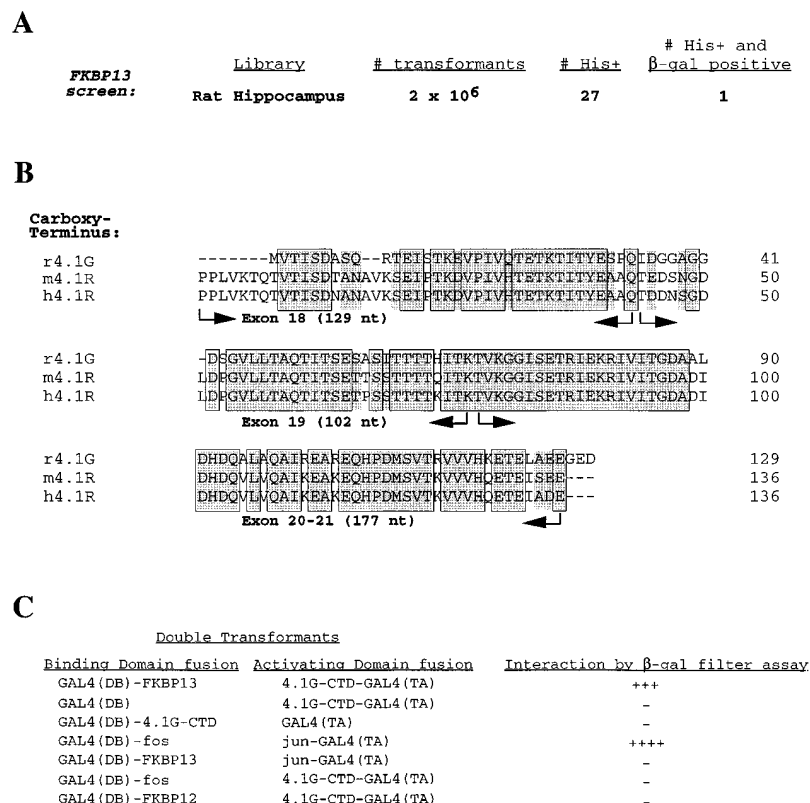
Figure 1. FKBP13 yeast two–hybrid screen. (*A*) Y190 yeast were transformed with a rat hippocampal library and 2×10^6 transformants were screened for his and β-gal activity. Whereas 27 colonies were his positive, a single colony was both his and β-gal positive. (*B*) The deduced aa sequence of the clone derived from the β-gal–positive colony is 71% identical to the corresponding region of the 4.1R–CTD encoded by exons 18–21 of the 4.1R gene. (The domains of 4.1R were originally defined by chymotryptic digestion [40], and thus, the CTD of 4.1R technically begins 11 aa upstream of exon 18; in this study, 4.1G–CTD refers to the 129-aa COOH-terminal peptide identified by yeast two-hybrid experiments.) Amino acid identities shared by r4.1G, m4.1R, and h4.1R are boxed and shaded, whereas conservative aa substitutions are shaded only. (*C*) Control experiments were performed using yeast doubly transformed with combinations of FKBP13 or 4.1G–CTD and the GAL4(DB) alone, the GAL4(TA) alone, and fos and jun constructs. A potential interaction between 4.1G–CTD and FKBP12 was also evaluated. Time (*t*) to positive β-gal signal in hours: $++++ = t \leq 0.25$; $+++ = 0.25 \leq t \leq 1$; $++ = 1 \leq t \leq 6$; $+ = 6 \leq t \leq 12$; $- =$ negative assay.
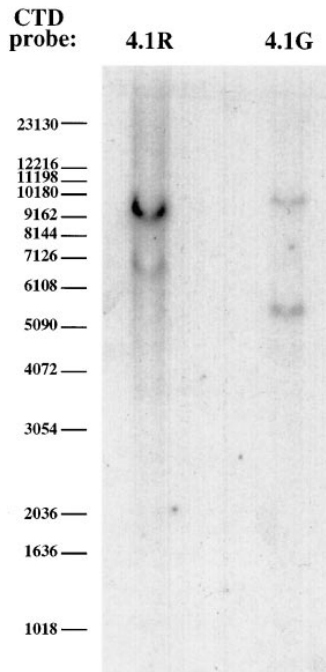
Figure 2. CTDs of 4.1G and 4.1R are encoded by distinct genes. Southern analysis of BamH1-digested rat genomic DNA yielded bands of 9.0 and 6.5 kb when hybridized with the 4.1R-CTD probe, and bands of 9.8 and 5.6 kb when incubated with the 4.1G–CTD probe.

two-hybrid experiments performed with 4.1G–CTD and FKBP12.

To determine if 4.1G–CTD is encoded by a distinct gene from 4.1R, Southern analysis was performed using rat genomic DNA digested with BamH1 and then incubated with 4.1R– and 4.1G–CTD probes (Fig. 2). Although the 4.1R–CTD probe hybridized with two bands of 9.0 and 6.5 kb, the 4.1G–CTD probe detected two bands of 9.8 and 5.6 kb. This finding indicates that 4.1G–CTD represents a distinct gene and thus, is a novel member of the 4.1R superfamily.

The complete m4.1G cDNA was obtained by sequencing overlapping EST clones and RT-PCR products (Fig. 3 *A*). The sequence was confirmed by high fidelity RT-PCR using two different cDNA sources and two nondegenerate primer pairs that generated overlapping products covering the complete cDNA (Fig. 3 *A*). The starting methionine was assigned on the following basis: (*a*) it is preceded by an in frame stop codon, (*b*) it is located in the context of a Kozak translation initiation sequence (-6 to $+4$ = GTAACCATGA), and (*c*) it encodes the MTTE motif that initiates the 135-kD isoform of 4.1R (14, 35). m4.1G is a 988-aa protein with a predicted mol wt of 110 kDa, and is 53% identical to m4.1R (Fig. 3 *B*). m4.1G sequences corresponding to the MBD, SABD, and CTD of m4.1R are

A

B
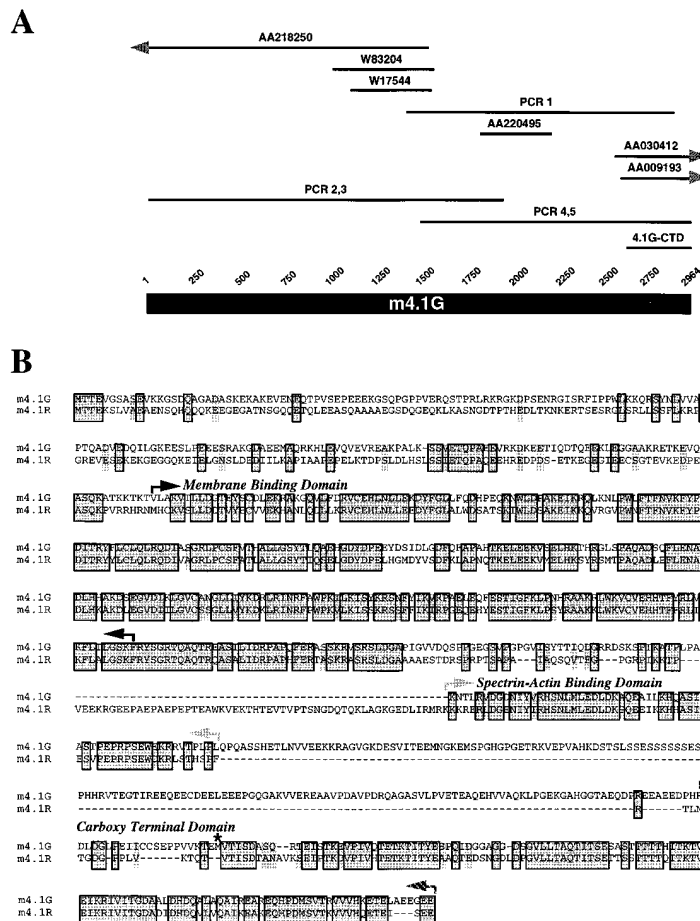
Figure 3. Identification and aa sequence of m4.1G. (*A*) The m4.1G cDNA was identified by double-strand sequencing of overlapping EST clones and RT-PCR products. The schematic demonstrates how the m4.1G cDNA was assembled: (*from top left*) *AA218250 (1–1521), W83204 (1030–1533), W17544 (1162–1528), PCR 1 (1441–2907), AA220495 (1807–2173), AA030412 (2554–2964), AA009193 (2575–2964).* Whereas EST clone AA218250 extends into the 5′ untranslated region (*left gray arrowhead*), clones AA030412 and AA009193 extend into the 3′ untranslated region (*right gray arrowhead*). The sequence was confirmed by high-fidelity RT-PCR using two different cDNA sources and two nondegenerate primer pairs that generated overlapping products covering the complete cDNA (*PCR 2,3: 1–1977* and *PCR 4,5: 1441–2964*). The corresponding location of the rat peptide identified in the yeast two-hybrid screen (*4.1G–CTD*) is also indicated. (*B*) The m4.1G cDNA encodes a protein of 988 aa with a predicted molecular weight of 110 kD. An aa-alignment of m4.1G and m4.1R highlights the identical sequence shared by the two proteins (*boxed* and *shaded portions*) and residues with conservative aa changes (*shaded portions*). m4.1G is 53% identical to m4.1R at the aa level, with 70, 68, and 64% aa identities in the MBD (*black arrows*), SABD (*gray arrows*), and CTD (*striped arrows*), respectively. The location of 4.1G–CTD is marked by an asterisk and occurs 30 aa beyond the start of the 4.1R–CTD, whose boundaries were originally defined by chymotryptic digests of 4.1R (40). m4.1G and m4.1R sequences diverge at the NH_2 termini and in regions separating the defined domains. Whereas there is increased m4.1R sequence between the MBD and SABD, the region between the SABD and CTD is expanded in m4.1G. m4.1G sequence data is available from EMBL/GenBank/DDBJ accession number AF044312.

highly conserved, with aa identities of 70, 68, and 64%, respectively. Discrete spans of divergence are located at the NH_2 termini (16% identity) and in the regions separating the defined domains. In addition, m4.1G exhibits 80% aa identity to the human 4.1G (h4.1G) isolated concurrently in our laboratories in a study of nonerythroid 4.1 species (47). Sequencing of PCR products and EST clones further revealed that, like 4.1R, 4.1G has multiple splice forms (data not shown).

Specificity of the FKBP13/4.1G–CTD Interaction

Whereas FK506 stimulates the binding of FKBP12 to calcineurin (42), stoichiometric quantities of FK506 dissociate FKBP12 from the ryanodine and IP_3 receptors (11, 36). Sequence motifs in the calcium channels are believed to mimic the structure of FK506, and thus compete with FK506 at the FKBP12 binding pocket (9). If FK506 and 4.1G–CTD likewise bind FKBP13 at the same site, the FKBP13/4.1G–CTD interaction should be blocked by FK506, thereby confirming the specificity of the interaction. This hypothesis was tested using the two-hybrid system by growing FKBP13 and 4.1G–CTD double transformants on plates containing 1, 10, and 50 μM of FK506 and then assessing β-gal activity compared to yeast grown on control plates (Fig. 4 A). The time required to detect β-gal activity increased with the dose of FK506, and with 50 μM FK506 no activity was observed. Thus, increasing doses of FK506 specifically block the FKBP13/4.1G–CTD interaction, presumably by saturating the expressed FKBP13. In yeast doubly transformed with fos and jun and grown on plates containing the three concentrations of FK506, no affect on β-gal activity was observed.

In vitro binding experiments further demonstrate the specificity of the FKBP13/4.1G–CTD interaction (Fig. 4 B). T7 his–FKBP13 bound to a GST–4.1G–CTD column and the interaction was inhibited by pretreating the FKBP13 lysate with 50 μM FK506. By contrast, T7 his–FKBP12 did not bind to the GST–4.1G–CTD column. FKBP13/4.1G–CTD binding was likewise demonstrated when T7 his–4.1G–CTD was incubated with a GST–FKBP13 column.

To test whether FKBP13 and 4.1G–CTD interact in mammalian cells, coimmunoprecipitation experiments were performed. HEK293 cells were transfected with NH_2-terminal c-myc–tagged 4.1G–CTD with or without COOH-terminal HA-tagged FKBP13. Immunoprecipitation with mouse monoclonal HA antibody, followed by Western analysis with affinity-purified mouse monoclonal c-myc antibody, demonstrated coimmunoprecipitation of c-myc–4.1G–CTD in the presence but not in the absence of HA–FKBP13 (Fig. 4 C).

Identification of the FKBP13 Binding Site on 4.1G–CTD

FKBP12 and FKBP13 are peptidyl-prolyl isomerases that bind FK506 and rapamycin with differing affinities (27). Because 4.1G–CTD binds to FKBP13 but not to FKBP12, we were interested in identifying the aa sequence that interacts with FKBP13 to shed light on the differing specificities of FKBP12 and FKBP13. Leu-pro and val-pro residues are optimal substrates for FKBP12 rotamase activity
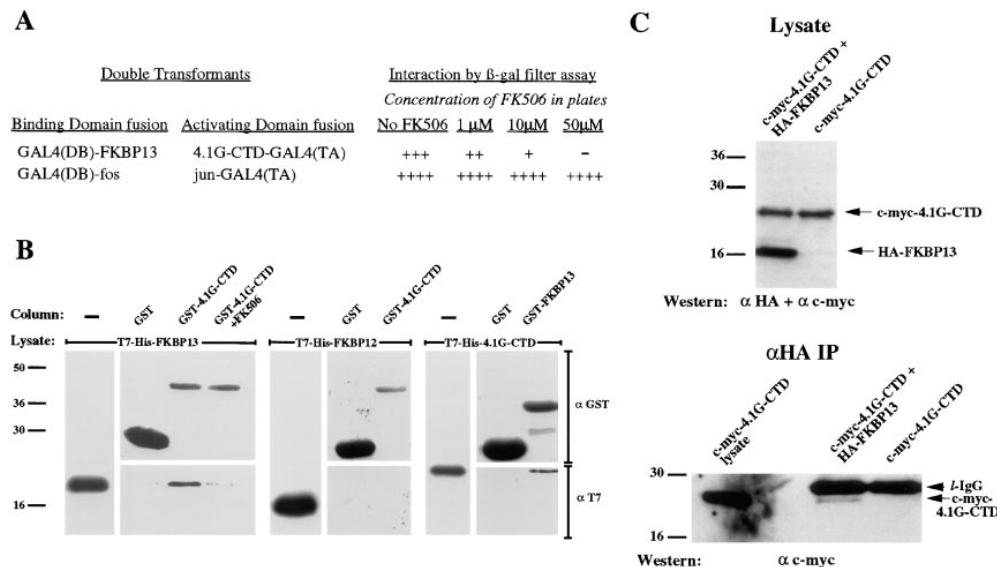

Figure 4. Specificity of the FKBP13/4.1G–CTD interaction. (*A*) FKBP13 and 4.1G–CTD double transformants were grown on plates containing 0, 1, 10, and 50 μM FK506. Fos and jun double transformants served as a positive control. The FKBP13/4.1G–CTD interaction, as assayed by β-gal filter assay, was inhibited by FK506 in a dose-dependent manner with complete blockage at 50 μM; the fos–jun interaction was unaffected by FK506. Time (*t*) to positive β-gal signal in hours: $++++ = t \leq 0.25$; $+++ = 0.25 \leq t \leq 1$; $++ = 1 \leq t \leq 6$; $+ = 6 \leq t \leq 12$; $- =$ negative assay. (*B*) In vitro binding experiments were conducted by incubating T7 his–FKBP13 lysate with a GST–4.1G–CTD matrix (*left*), T7 his–FKBP12 lysate with a GST–4.1G–CTD matrix (*middle*), and T7 his–4.1G–CTD lysate with a GST–FKBP13 matrix (*right*). Whereas T7 his–FKBP13 bound to the GST–4.1G–CTD matrix, T7 his-FKBP12 did not. The T7 his–FKBP13 binding was blocked by 50 μM FK506. FKBP13/4.1G–CTD binding also occurred when the fusions were switched (*right*). (*C*) (*Top*) HEK293 cells were transfected with NH_2-terminal c-myc–tagged 4.1G–CTD with or without COOH-terminal HA-tagged FKBP13, and then lysates were subjected to Western analysis using a mixture of anti-HA and anti–c-myc monoclonal antibodies (*top*). (*Bottom*) Incubation of the lysates with mouse monoclonal HA antibody resulted in coimmunoprecipitation of c-myc–4.1G–CTD (*arrow*) with HA–FKBP13. c-myc–4.1G–CTD is not detected when anti-HA immunoprecipitation is conducted using lysates containing c-myc–4.1G–CTD alone. The arrowhead indicates the band corresponding to light chain IgG (*l-IgG*). Western blot exposures were kept short (5–20 s) so that the immunoprecipitated band could be resolved from the robust *l*-IgG band.

in vitro (1); FK506 binds with high affinity to FKBP12 and inhibits its rotamase activity by mimicking the transition state of peptidyl-prolyl isomerization. Leu-pro 1400–1401 of the IP$_3$ receptor has recently been shown to mediate the constitutive binding of FKBP12 to the calcium channel and presumably has structural characteristics similar to FK506 (9).

4.1G–CTD contains three peptidyl-prolyl bonds that could potentially participate in FKBP13 binding, including val-pro at aa 18–19, ser-pro at 32–33, and his-pro at 107–108. We used yeast two–hybrid assays to determine which residues are required for the FKBP13 interaction. Yeast were doubly transformed with FKBP13 and truncations of 4.1G–CTD corresponding to aa 1–67 and 35–129. Only the transformants containing the 35–129 aa-construct exhibited β-gal activity, which occurred with the same time course as yeast transformed with the complete 4.1G–CTD (Fig. 5). The inability of the 1–67 aa construct to produce β-gal activity, eliminated val-pro and ser-pro as FKBP13 targets. To determine if the his-pro was responsible for FKBP13 binding, a 4.1G–CTD construct containing aa 1–106 that lacks this moiety and two constructs containing pro 108 to ala mutations (1–129:P108A and 35–129:P108A) were evaluated. These modifications completely abolished the FKBP13 interaction measured in yeast two-hybrid assays, suggesting that pro 108 of 4.1G–CTD is important for FKBP13 binding. The finding that a pro preceded by his is involved in the interaction (rather than a leu- or val-pro), prompted us to assess whether his 107 is required for binding. 4.1G–CTD constructs containing his 107 to leu (1-129:H107L) and his 107 to arg (1–129:H107R) mutations both failed to promote the FKBP13/4.1G–CTD interaction in yeast two–hybrid assay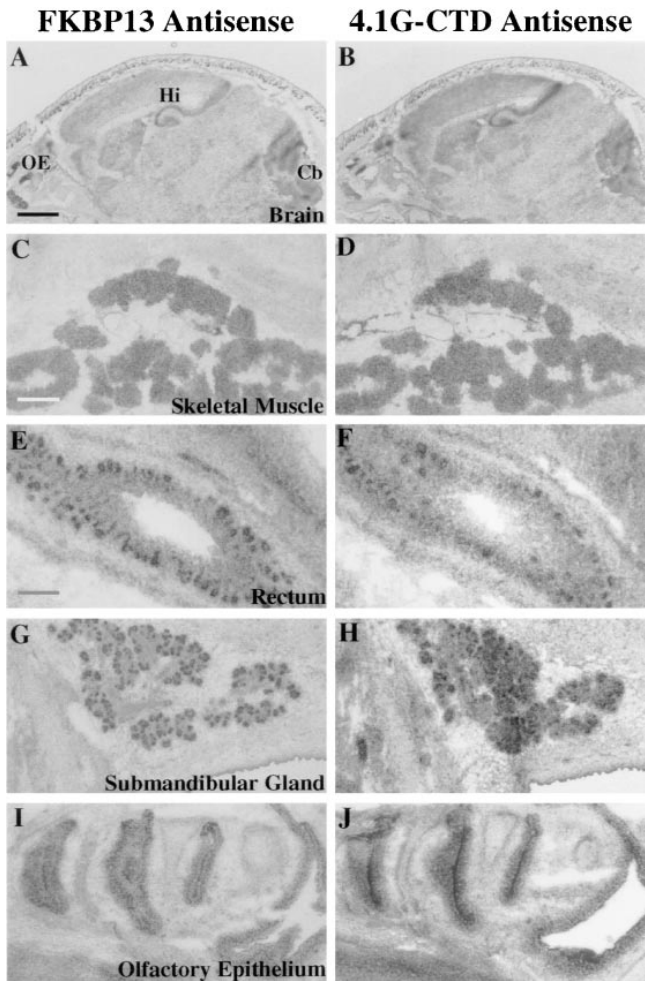s. His-pro 107–108 may confer bind-ing specificity through direct interaction with FKBP13 or by generating/stabilizing a requisite secondary structure.

Colocalization of FKBP13 and 4.1G–CTD In Vivo

Whereas protein 4.1 has been identified in a wide range of tissues by immunologic methods (19, 24, 30, 54), the discovery of a new homologue indicates that protein 4.1 localizations in the body should be redefined in an isotype-specific manner. In situ hybridization studies of E18 rat embryos and 4-d-old newborn mice demonstrated 4.1G–CTD–containing mRNAs in a wide variety of tissues including the central nervous system, olfactory epithelium, toothbuds, skeletal muscle, salivary glands, thymus, thy-
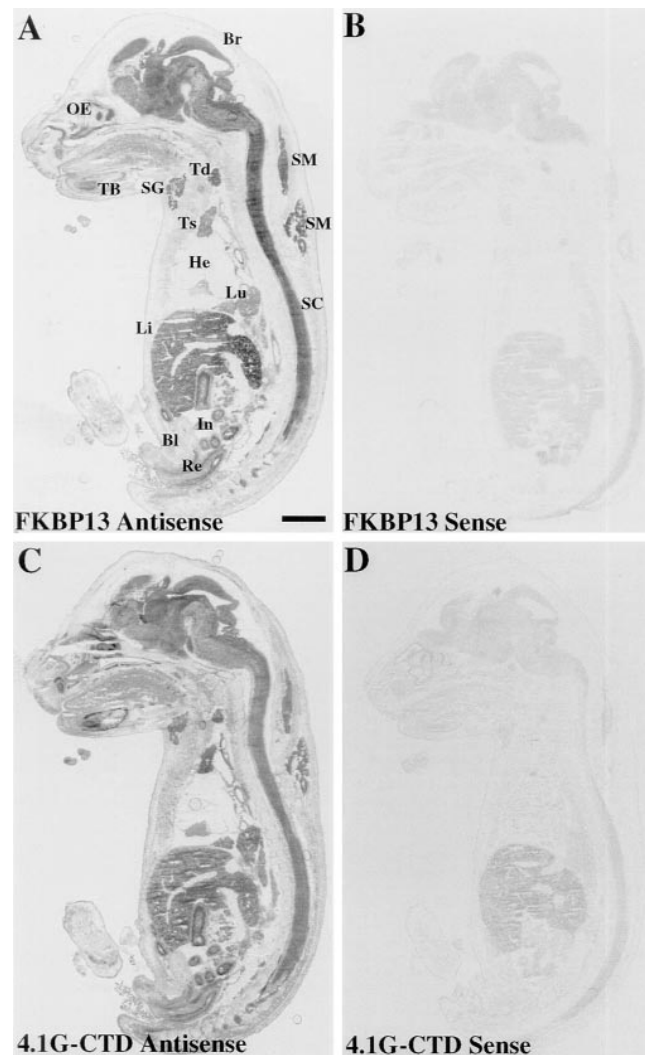
Figure 6. Colocalization of FKBP13 with 4.1G–CTD in E18 rat embryos. In situ hybridization identified FKBP13 and 4.1G–CTD–containing mRNAs in identical distributions during embryonic development (*A* and *C*). Colocalizations identifiable at low power include the brain (*Br*), spinal cord (*SC*), olfactory epithelium (*OE*), submandibular gland (*SG*), thymus (*Ts*), thyroid (*Td*), skeletal muscle (*SM*), lung (*Lu*), liver (*Li*), intestines (*In*), and rectum (*Re*). No signal is detected, for example, in heart (*He*) or bladder (*Bl*). The specific in situ hybridization signals are absent in control sections incubated with FKBP13 and 4.1G–CTD sense cRNAs (*B* and *D*). Bar, 2.1 mm.

Figure 5. Identification of the FKBP13 binding site. Truncations of 4.1G–CTD were evaluated for interaction with FKBP13 in yeast by β-gal filter assay. A positive interaction using the 35–129-aa construct implicated pro 108 in FKBP13 binding. The requirement of pro 108 was confirmed using a construct truncated immediately upstream of pro 108 (1–106) and two constructs containing a pro 108 to ala mutation; all three constructs failed to produce β-gal activity. 4.1G–CTD constructs containing his 107 to leu (1–129:H107L) and his 107 to arg (1–129:H107R) mutations also failed to produce a positive β-gal signal. Time (*t*) to positive β-gal signal in hours: $++++ = t \leq 0.25$; $+++ = 0.25 \leq t \leq 1$; $++ = 1 \leq t \leq 6$; $+ = 6 \leq t \leq 12$; $- =$ negative assay.

FKBP13 Antisense   **4.1G-CTD Antisense**

Figure 7. Examples of the FKBP13/4.1G–CTD colocalization within specific tissues during development. (*A* and *B*) FKBP13 and 4.1G–CTD–containing mRNAs colocalize in the olfactory epithelium (*OE*), hippocampus (*Hi*), and cerebellum (*Cb*) of 4-d-old mice. High-power images of E18 rat embryos demonstrate colocalizations in skeletal muscle bundles (*C* and *D*), crypts of Leiberkuhn in the rectum (*E* and *F*), secretory epithelium of the submandibular gland (*G* and *H*), and olfactory epithelium (*I* and *J*). Bars: (*A* and *B*) 1.30 mm; (*C, D, G,* and *H–J*) 0.32 mm; (*E* and *F*) 0.16 mm.

roid, spleen, bone marrow, liver, lung, intestine, adrenal, and testis (Fig. 6 *C*, Fig. 7, and data not shown). In contrast, 4.1R mRNAs were selectively localized in these sections to hematopoietic tissues and discrete neuronal populations (Walensky, L.D., Z.T. Shi, S. Blackshaw, A.C. DeVries, G.E. Demas, P. Gascard, R.J. Nelson, J.G. Conboy, E.M. Rubin, S.H. Snyder, and N. Mohandas. 1997. *Mol. Biol. Cell* [*Suppl.*] 8:275a). FKBP13 colocalized with 4.1G–CTD throughout the body of E18 rat embryos (Fig. 6). At low power, high levels of FKBP13 and 4.1G–CTD mRNAs were evident in the brain, spinal cord, olfactory tissue, salivary glands, thyroid, thymus, skeletal muscle, lung, liver, intestines, and rectum (Fig. 6, *A* and *C*). There was negligible expression in heart, bladder, blood vessels, and intestinal smooth muscle. Higher power images revealed colocalizations of FKBP13 and 4.1G–CTD in hippocampus and cerebellum of the developing brain, skeletal muscle bun-

dles, crypts of the rectal mucosa, salivary gland epithelium, and olfactory epithelium, for example (Fig. 7).

Identification of FKBP13 in RBC Ghost Preparations

We investigated whether FKBP13 occurs in RBCs for the following reasons: (*a*) the CTDs of 4.1G and 4.1R are highly conserved in the defined FKBP13 binding region; (*b*) RBCs are one of the most abundant sources of 80-kD 4.1R in the body (16); (*c*) in situ hybridization studies revealed that 4.1G mRNAs also localize to hematopoietic tissues; and (*d*) because RBCs lack ER, we could determine if FKBP13 is found outside of the ER in association with the membrane cytoskeleton. Rat RBCs were purified from whole blood and then hemoglobin-free cytosol and ghost fractions were isolated. Whereas 4.1R is not present in the cytosol of RBCs, it is highly enriched in the ghost fraction (5). RBC ghosts are produced by hypotonic lysis of RBCs followed by extensive washing, and represent the intact membrane and cytoskeletal structure of RBCs without cytosolic contents. Affinity-purified polyclonal antibodies that specifically recognize FKBP12 or FKBP13 (Fig. 8 *A*) identified FKBP12 exclusively in the RBC cytosol fraction, and FKBP13 solely in the ghost fraction (Fig. 8 *B*). Brain extracts served as positive controls for Western analysis. To confirm that the protein identified in RBC ghosts has FK506 binding activity, ghosts were solubilized and then incubated with an FK506 matrix in the presence or absence of soluble FK506, which should block binding. Bound proteins were eluted from the matrix with SDS sample buffer, electrophoresed, and then subjected to FKBP12 and FKBP13 Western analysis. The FKBP13 antibody recognized a 13-kD protein from solubilized ghosts that bound to the FK506 matrix and was specifically displaced by free FK506 (Fig. 8 *C*). In contrast, the FKBP12 antibody did not recognize any proteins extracted from the ghost preparation.

We subfractionated RBC ghosts to determine if FKBP13 segregates with 4.1R (Fig. 8 *D*). Western analysis of the preparations was conducted using the FKBP13 antibody (Fig. 8 *D*, *bottom panel*) and an affinity-purified anti-4.1R peptide antibody (18) (*top panel*). IOVs that are depleted of spectrin and actin retained 4.1R (80-kD doublet [17]) and FKBP13. IOVs that are then depleted of peripheral membrane proteins by a stripping procedure lose 4.1R and FKBP13. Finally, Triton shells were prepared from RBC ghosts to further enrich for 4.1R. Western analysis of this preparation demonstrated increased amounts of 4.1R. The quantity of FKBP13 in Triton shells was likewise enriched compared to ghosts and IOVs.

It should be noted that these experiments do not completely rule out the possibility that the 13-kD protein identified in RBC ghosts is a distinct immunophilin that is recognized by the FKBP13 antibody and comigrates with brain FKBP13.

Discussion

In the present study we have identified 4.1G–CTD as the first known binding target of FKBP13. 4.1G is a novel, widely expressed homologue of the erythrocyte membrane cytoskeletal protein (4.1R). The FKBP13/4.1G–
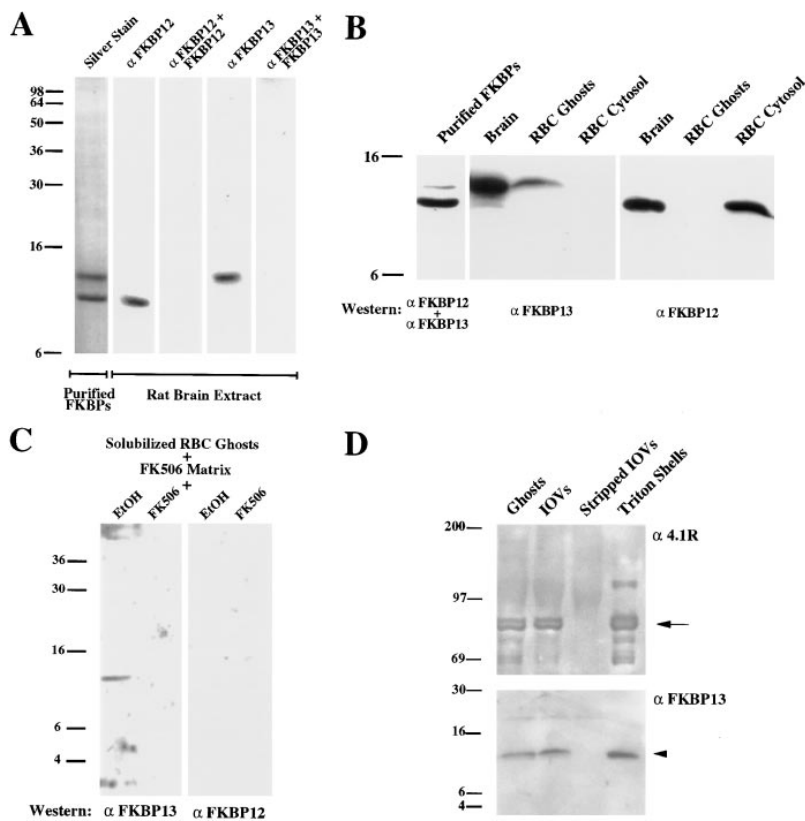
Figure 8. Identification of FKBP13 in RBC ghost preparations. (*A*) Affinity-purified FKBP12 and FKBP13 antibodies selectively recognize the corresponding FKBPs in brain extracts. The signals are blocked by preincubating the antibodies with the respective FKBP fusion proteins. A silver stain of FKBPs purified from brain using an FK506 matrix served as FKBP molecular weight markers. (*B*) RBCs were purified from whole blood and then hemoglobin-free cytosol and ghosts were isolated. FKBP antibodies detected FKBP13 in ghosts but not in cytosol, whereas FKBP12 was identified in cytosol but not in ghosts. Brain extract served as a positive control for Western analysis. (*C*) Solubilized RBC ghosts were incubated with an FK506 matrix in the presence of vehicle (2% ethanol) alone or 100 µM FK506. The FKBP13 antibody recognized a 13-kD protein from solubilized ghosts that bound to the FK506 matrix and was completely competed by soluble FK506. In contrast, the FKBP12 antibody did not recognize any proteins isolated from the ghosts. (*D*) RBC ghosts, IOVs, stripped IOVs, and Triton shells were prepared and subjected to Western analysis using 4.1R (*top*) and FKBP13 (*bottom*) antibodies. Whereas 4.1R (80-kD doublet [17], *arrow*) and FKBP13 (*arrowhead*) are present in ghosts and IOVs, the proteins are absent from stripped IOVs. Triton shells are enriched with 80 kD–4.1R and other bands recognized by the antibody, including the 135-kD isoform of 4.1R and lower molecular weight splice forms or breakdown products (17, 39). Triton shells likewise have an increased amount of FKBP13 compared to ghost and IOV samples.

CTD interaction was discovered using the yeast two–hybrid system and then confirmed by in vitro binding and coimmunoprecipitation studies. Specificity of the association was established by blocking in vitro binding and the yeast interaction with FK506.

The cyclophilin and FKBP immunophilins possess peptidyl-prolyl isomerase activity, which interconverts the *cis* and *trans* isomers of peptidyl-prolyl bonds (33, 51). FK506 mimics the transition state of peptidyl-prolyl isomerization, and thus effectively competes with natural substrates for FKBP binding. Interestingly, the binding domains of FKBP12 and FKBP13 for FK506 are virtually superimposable, as determined by X-ray crystallographic studies (53). However, the respective K_is of FK506 and rapamycin are 0.6 and 0.26 nM for FKBP12, and 74 and 3 nM for FKBP13 (27), suggesting that the two proteins may have different substrate specificities in vivo. The differences between the affinities of FKBP12 and FKBP13 for FK506 and rapamycin have been explained by the cumulative effect of multiple small distortions in their protein structures (53). Another distinction between the binding properties of FKBP12 and FKBP13 is exemplified by the ability of FKBP12, but not FKBP13, to form a complex with calcineurin in the presence of FK506. The inability of FKBP13–FK506 to interact with calcineurin is attributed to the distinct gln-50, ala-95, and lys-98 surface residues of FKBP13 (27).

The binding of 4.1G–CTD to FKBP13 but not to FKBP12 underscores the selective nature of immunophilin interactions in vivo. Protein motifs that mimic the transition state of peptidyl-prolyl isomerization are believed to produce high affinity, steady-state interactions with FKBPs (9). In this study, we have determined that his-pro 107–108 of 4.1G–CTD is required for FKBP13 binding. The crystallographic structure of the FKBP12–FK506 complex indicates that the leu-like moiety of FK506, the pyranose methyl group region, shares a complementary surface with the side chains of his-87 and ile-91 of FKBP12. The corresponding aa in FKBP13 are ala-95 and lys-98. There is predicted complementarity between the IP$_3$R-leu 1401 and FKBP12–his 87 in the FKBP12–IP$_3$R complex (9); the analogous aliphatic and his residues are reversed in FKBP13 and 4.1G–CTD, suggesting that the 4.1G–CTD–his 107 may interface with FKBP13–ala 95. We speculate that an aliphatic–his complementarity may participate in FKBP-substrate interactions in vivo, conferring FKBP specificity based on the residues preceding pro in the physiologic targets.

A physiologic role for the FKBP13/4.1G–CTD interaction is supported by the striking tissue colocalizations demonstrated throughout the body during development by in situ hybridization. FKBP13 and 4.1G–CTD-containing mRNAs are widely expressed with enrichment in skeletal muscle, salivary glands, and the gastrointestinal, hematopoietic, respiratory, and nervous systems. Within these tissues, the proteins colocalize, for example, in intestinal crypt, salivary gland, and olfactory epithelium. Areas

where expression of both transcripts is negligible include the heart and smooth muscle tissue of the gastrointestinal tract, urinary bladder, and blood vessels. Whereas 4.1R transcripts predominantly localize to hematopoietic tissues and select neuronal populations (Walensky, L.D., Z.T. Shi, S. Blackshaw, A.C. DeVries, G.E. Demas, P. Gascard, R.J. Nelson, J.G. Conboy, E.M. Rubin, S.H. Snyder, and N. Mohandes. 1997. *Mol. Biol. Cell* [*Suppl.*] 8:275a), 4.1G mRNAs are broadly distributed, indicating a more generalized role for this 4.1 homologue.

The strong homology between 4.1G and 4.1R suggests that the novel 4.1G gene encodes a membrane cytoskeletal protein. The primary structure of FKBP13, however, contains a putative signal sequence and a variant of the defined KDEL motif, which may serve to target and retain FKBP13 in the ER, respectively (37). The identification of a specific binding interaction between FKBP13 and 4.1G–CTD, coupled with their mRNA tissue colocalizations, suggested that FKBP13 may additionally be found outside of the ER in association with 4.1G in the membrane cytoskeleton. Whereas FKBP13 has been identified in rough microsomal fractions enriched with ER membrane and luminal proteins (46), we were interested in determining if the membrane cytoskeleton could be a further source of FKBP13 protein. Thus, we conducted FKBP Western analysis on purified RBCs because they lack ER and are enriched in 4.1R, which shares sequence identity with 4.1G in the region implicated in FKBP13 binding. FKBP12 (38) and a 12-kD inositol phosphate-binding protein (22), believed to be an immunophilin, have previously been identified in RBCs. Our affinity-purified FKBP antibodies identified FKBP12 in the cytosol of RBCs and FKBP13 in RBC ghosts, where 4.1R is located. In addition, FKBP13 can be extracted from solubilized ghosts on the basis of its affinity for an FK506 matrix. Ghosts stripped of actin and spectrin retain both FKBP13 and 4.1R, whereas further treatment to remove peripheral membrane proteins liberates FKBP13 and 4.1R from the vesicles. The Triton shell preparation that enriches for 4.1R likewise contains increased FKBP13 compared to ghost and IOV samples. The development of isoform-specific antibodies is required to determine if 4.1G is found in RBCs and if the FKBP13 of RBCs interacts with 4.1G and/or 4.1R. These results demonstrate, however, that FKBP13 is a component of the RBC membrane cytoskeleton, and thus can occur outside of the ER. FKBP13 may localize to two distinct subcellular compartments by alternate transcriptional, translational or posttranslational processing of its putative NH_2-terminal targeting sequence.

Whereas functional interactions of the MBD and SABD of 4.1R have been well documented (21, 44), the role of the CTD remains undefined. In this report, we demonstrate the binding of FKBP13 to the CTD of 4.1G. What functional role might FKBP13 play in association with 4.1G–CTD? Some clues may be derived from the physiologic implications of FKBP12 binding to its cellular targets. For example, FKBP12 has recently been shown to anchor calcineurin to the IP_3 receptor in a ternary complex, which regulates the phosphorylation state and function of the calcium channel (10). FKBP12 may serve a similar anchoring function in its association with the TGFβ type 1 family of receptors (57, 58). By analogy, FKBP13 may anchor

regulatory protein phosphatases (or kinases) to 4.1G–CTD, which may in turn regulate 4.1G function. 4.1R is well known to be phosphorylated in vitro and in vivo by protein kinase A, protein kinase C, and casein kinase II (13); in each case, 4.1R phosphorylation leads to a marked decrease in its ability to bind spectrin and promote the spectrin–actin interaction (13). In addition, protein kinase C phosphorylation of 4.1R inhibits its binding to membranes by blocking the interaction with band 3 (23).

In summary, our studies have identified a novel 4.1 homologue, whose CTD is a specific binding partner for immunophilin FKBP13. Interestingly, the 4.1G–CTD peptide sequence required for FKBP13 binding is conserved in 4.1R across species. Research into the physiologic implications of the FKBP13/4.1G–CTD interaction may provide insight into the functional role of the CTD of 4.1 proteins. The identification of FKBP13 outside of the ER, coupled with the widespread expression and colocalization of FKBP13 and 4.1G–CTD transcripts throughout the body during development, suggest that these proteins perform a generalized function in the membrane cytoskeleton of mammalian cells.

References

1. Albers, M.W., C.T. Walsh, and S.L. Schreiber. 1990. Substrate specificity for the human rotamase FKBP: a view of FK506 and rapamycin as leucine-(twisted amide)-proline mimics. *J. Org. Chem.* 55:4984–4986.
2. Alloisio, N., N. Dalla Venezia, A. Rana, K. Andrabi, P. Texier, F. Gilsanz, J.P. Cartron, J. Delaunay, and A.H. Chishti. 1993. Evidence that red blood cell protein p55 may participate in the skeleton-membrane linkage that involves protein 4.1 and glycophorin C. *Blood.* 82:1323–1327.
3. Ausubel, F.M., R. Brent, R.E. Kingston, D.D. Moore, J.G. Seidman, J.A. Smith, and K. Struhl. 1990. Current Protocols in Molecular Biology. John Wiley, New York.
4. Baklouti, F., S.C. Huang, T.J. Vulliamy, J. Delaunay, and E.J. Benz, Jr. 1997. Organization of the human protein 4.1 genomic locus: new insights into the tissue-specific alternative splicing of the pre-mRNA. *Genomics.* 39:289–302.
5. Bennett, V. 1983. Proteins involved in membrane-cytoskeleton association in human erythrocytes: spectrin, ankyrin and band 3. *Methods Enzymol.* 96:313–324.
6. Beutler, E., C. West, and K.G. Blume. 1976. The removal of leukocytes and platelets from whole blood. *J. Lab. Clin. Med.* 88:328–333.
7. Blackshaw, S., and S.H. Snyder. 1997. Developmental expression pattern of phototransduction components in mammalian pineal implies a light-sensing function. *J. Neurosci.* 17:8074–8082.
8. Bush, K.T., B.A. Henrickson, and S.K. Nigam. 1994. Induction of the FK506-binding protein, FKBP13, under conditions which misfold proteins in the endoplasmic reticulum. *Biochem. J. (Tokyo).* 303:705–708.
9. Cameron, A.C., F.C. Nucifora, E.T. Fung, D.J. Livingston, R.A. Aldape, C.A. Ross, and S.H. Snyder. 1997. FKBP12 binds the inositol 1,4,5-tris-

phosphate receptor at leucine-proline (1400-1401) and anchors calcineurin to this FK506-like domain. *J. Biol. Chem.* 272:27582–27588.

10. Cameron, A.M., J.P. Steiner, A.J. Roskams, S.M. Ali, G.V. Ronnett, and S.H. Snyder. 1995. Calcineurin associated with the inositol 1,4,5-trisphosphate receptor-FKBP12 complex modulates Ca^{2+} flux. *Cell.* 83:463–472.

11. Cameron, A.M., J.P. Steiner, D.M. Sabatini, A.I. Kaplin, L.D. Walensky, and S.H. Snyder. 1995. Immunophilin FK506 binding protein associated with inositol 1,4,5-trisphosphate receptor modulates calcium flux. *Proc. Natl. Acad. Sci. USA.* 92:1784–1788.

12. Chevray, P.M., and D. Nathans. 1992. Protein interaction cloning in yeast: Identification of mammalian proteins that react with the leucine zipper of Jun. *Proc. Natl. Acad. Sci. USA.* 89:5789–5793.

13. Cohen, C.M., and P. Gascard. 1992. Regulation and post-translational modification of erythrocyte membrane and membrane-skeletal proteins. *Sem. Hematol.* 29:244–292.

14. Conboy, J., Y.W. Kan, S.B. Shohet, and N. Mohandas. 1986. Molecular cloning of protein 4.1, a major structural element of the human erythrocyte membrane skeleton. *Proc. Natl. Acad. Sci. USA.* 83:9512–9516.

15. Conboy, J.G. 1993. Structure, function, and molecular genetics of erythroid membrane skeletal protein 4.1 in normal and abnormal red blood cells. *Semin. Hematol.* 30:58–73.

16. Conboy, J.G., J. Chan, N. Mohandas, and Y.W. Kan. 1988. Multiple protein 4.1 isoforms produced by alternative splicing in human erythroid cells. *Proc. Natl. Acad. Sci. USA.* 85:9062–9065.

17. Conboy, J.G., J.Y. Chan, J.A. Chasis, Y.W. Kan, and N. Mohandas. 1991. Tissue- and development-specific alternative RNA splicing regulates expression of multiple isoforms of erythroid membrane protein 4.1. *J. Biol. Chem.* 266:8273–8280.

18. Conboy, J.G., R. Shitamoto, M. Parra, R. Winardi, A. Kabra, J. Smith, and N. Mohandas. 1991. Hereditary elliptocytosis due to both qualitative and quantitative defects in membrane skeletal protein 4.1. *Blood.* 78:2438–2443.

19. Constantinescu, E., C. Heltianu, and M. Simionescu. 1986. Immunological detection of an analogue of the erythroid protein 4.1 in endothelial cells. *Cell Biol. Int. Rep.* 10:861–868.

20. Correas, I., T.L. Leto, D.W. Speicher, and V.T. Marchesi. 1986. Identification of the functional site of erythrocyte protein 4.1 involved in spectrin-actin associations. *J. Biol. Chem.* 261:3310–3315.

21. Correas, I., D.W. Speicher, and V.T. Marchesi. 1986. Structure of the spectrin-actin binding site of erythrocyte protein 4.1. *J. Biol. Chem.* 261: 13362–13366.

22. Cunningham, E.B. 1995. The human erythrocyte membrane contains a novel 12-kDa inositolphosphate-binding protein that is an immunophilin. *Biochem. Biophys. Res. Commun.* 215:212–218.

23. Danilov, Y.N., R. Fennell, E. Ling, and C.M. Cohen. 1990. Selective modulation of band 4.1 binding to erythrocyte membranes by protein kinase C. *J. Biol. Chem.* 265:2556–2562.

24. Davies, G.E., and C.M. Cohen. 1985. Platelets contain proteins immunologically related to red cell spectrin and protein 4.1. *Blood.* 65:52–59.

25. Freinz, F., M.W. Albers, A. Galat, R.F. Standaert, W.S. Lane, S.J. Burakoff, B.E. Bierer, and S.L. Schreiber. 1991. Rapamycin and FK506 binding proteins (immunophilins). *J. Am. Chem. Soc.* 113:1409–1411.

26. Fruman, D.A., C.B. Klee, B.E. Bierer, and S.J. Burakoff. 1992. Calcineurin phosphatase activity in T lymphocytes is inhibited by FK 506 and cyclosporin A. *Proc. Natl. Acad. Sci. USA.* 89:3686–3686.

27. Futer, O., M.T. DeCenzo, R.A. Aldape, and D.J. Livingston. 1995. FK506 binding protein mutational analysis. *J. Biol. Chem.* 270:18935–18940.

28. Galat, A. 1993. Peptidylproline cis-trans-isomerases: immunophilins. *Eur. J. Biochem.* 216:689–707.

29. Gascard, P., and C.M. Cohen. 1994. Absence of high-affinity band 4.1 binding sites from membranes of glycophorin C- and D-deficient (Leach phenotype) erythrocytes. *Blood.* 83:1102–1108.

30. Goodman, S.R., L.A. Casoria, D.B. Coleman, and I.S. Zagon. 1984. Identification and location of brain protein 4.1. *Science.* 224:1433–1436.

31. Handschumacher, R.E., M.W. Harding, J. Rice, R.J. Drugge, and D.W. Speicher. 1994. Cyclophilin: a specific cytosolic binding protein for cyclosporin A. *Nature.* 226:544–546.

32. Harding, M.W., A. Galat, D.E. Uehling, and S.L. Schreiber. 1989. A receptor for the immunosuppressant FK506 is a cis-trans peptidyl-prolyl isomerase. *Nature.* 341:758–760.

33. Harrison, R.K., and R.L. Stein. 1990. Substrate specificities of the peptidyl prolyl cis-trans isomerase activities of cyclophilin and FK-506 binding protein: evidence for the existence of a family of distinct enzymes. *Biochemistry.* 29:3813–3816.

34. Horton, R.M., H.D. Hunt, S.N. Ho, J.K. Pullen, and L.R. Pease. 1989. Engineering hybrid genes without the use of restriction enzymes: gene splicing by overlap extension. *Gene.* 77:61–68.

35. Huang, J.P., C.J. Tang, G.H. Kou, V.T. Marchesi, E.J. Benz, Jr., and T.K. Tang. 1993. Genomic structure of the locus encoding protein 4.1. Structural basis for complex combinational patterns of tissue-specific alternative RNA splicing. *J. Biol. Chem.* 268:3758–3766.

36. Jayaraman, T., A.M. Brillantes, A.P. Timerman, S. Fleischer, H. Erdjument-Bromage, P. Tempst, and A.R. Marks. 1992. FK506 binding protein associated with the calcium release channel (ryanodine receptor). *J. Biol. Chem.* 267:9474–9477.

37. Jin, Y.J., M.W. Albers, W.S. Lane, B.E. Bierer, S.L. Schreiber, and S.J. Burakoff. 1991. Molecular cloning of a membrane-associated human FK506- and rapamycin-binding protein, FKBP-13. *Proc. Natl. Acad. Sci. USA.* 88:6677–6681.

38. Kay, J.E., E. Sampare-Kwateng, F. Geraghty, and G.Y. Morgan. 1991. Uptake of FK506 by lymphocytes and erythrocytes. *Transplant Proc.* 23:2760–2762.

39. Krauss, S.W., C.A. Larabell, S. Lockett, P. Gascard, S. Penman, N. Mohandas, and J.A. Chasis. 1997. Structural protein 4.1 in the nucleus of human cells: dynamic rearrangements during cell division. *J. Cell. Biol.* 137:275–289.

40. Leto, T.L., and V.T. Marchesi. 1984. A structural model of human erythrocyte protein 4.1. *J. Biol. Chem.* 259:4603–4608.

41. Li, X.J., S.H. Li, A.H. Sharp, F.C.J. Nucifora, G. Schilling, A. Lanahan, P. Worley, S.H. Snyder, and C.A. Ross. 1995. A huntingtin-associated protein enriched in brain with implications for pathology. *Nature.* 378:398–402.

42. Liu, J., J.D. Farmer, Jr., W.S. Lane, J. Friedman, I. Weissman, and S.L. Schreiber. 1991. Calcineurin is a common target of cyclophilin-cyclosporin A and FKBP-FK506 complexes. *Cell.* 66:807–815.

43. Liu, J., M.W. Albers, T.J. Wandless, S. Luan, D.G. Alberg, P.J. Belshaw, P. Cohen, C. MacKintosh, C.B. Klee, and S.L. Schreiber. 1992. Inhibition of T cell signaling by immunophilin-ligand complexes correlates with loss of calcineurin phosphatase activity. *Biochemistry.* 31:3896–3901.

44. Marfatia, S.M., R.A. Leu, D. Branton, and A.H. Chishti. 1995. Identification of the protein 4.1 binding interface on glycophorin C and p55, a homologue of the *Drosophila* discs-large tumor suppressor protein. *J. Biol. Chem.* 270:715–719.

45. McCombie, W.R., C. Heiner, J.M. Kelly, M.G. Fitzgerald, and J.D. Gocayne. 1992. Rapid and reliable fluorescent cycle sequencing of double stranded templates. *DNA Seq.* 2:289–296.

46. Nigam, S.K., Y.J. Jin, M.J. Jin, K.T. Bush, B.E. Bierer, and S.J. Burakoff. 1993. Localization of the FK506-binding protein, FKBP13, to the lumen of the endoplasmic reticulum. *Biochem. J. (Tokyo).* 294:511–515.

47. Parra, M., P. Gascard, L.D. Walensky, S.H. Snyder, N. Mohandas, and J.G. Conboy. 1998. Identification and characterization of a novel widely expressed homologue of the erythroid membrane skeletal protein 4.1. *Genomics.* In press.

48. Partaledis, J.A., and V. Berlin. 1993. The FKB2 gene of *Saccharomyces cerevisiae*, encoding the immunosuppressant-binding protein FKBP-13, is regulated in response to accumulation of unfolded proteins in the endoplasmic reticulum. *Proc. Natl. Acad. Sci. USA.* 90:5450–5454.

49. Pasternack, G.R., R.A. Anderson, T.L. Leto, and V.T. Marchesi. 1985. Interactions between protein 4.1 and band 3. An alternative binding site for an element of the membrane skeleton. *J. Biol. Chem.* 260:3676–3683.

50. Pow, D.V., and D.K. Crook. 1993. Extremely high titre polyclonal antisera against small neurotransmitter molecules: rapid production, characterization and use in light- and electron-microscopic immunocytochemistry. *J. Neurosci. Methods.* 48:51–63.

51. Rosen, M.K., R.F. Standaert, A. Galat, M. Nakatsuka, and S.L. Schreiber. 1990. Inhibition of FKBP rotamase activity by immunosuppressant FK506: twisted amide surrogate. *Science.* 248:863–866.

52. Sambrook, J., E.F. Fritsch, and T. Maniatis. 1989. Molecular Cloning: A Laboratory Manual. Cold Spring Harbor Laboratory Press, Cold Spring Harbor, New York. 545 pp.

53. Schultz, L.W., P.K. Martin, J. Liang, S.L. Schreiber, and J. Clardy. 1994. Atomic structure of the immunophilin FKBP13-FK506 complex: insights into the composite binding surface for calcineurin. *J. Am. Chem. Soc.* 116:3129–3130.

54. Sihag, R.K., L.W. Wang, A.M. Cataldo, M. Hamlin, C.M. Cohen, and R.A. Nixon. 1994. Evidence for the association of protein 4.1 immunoreactive forms with neurofibrillary tangles in Alzheimer's disease brains. *Brain Res.* 656:14–26.

55. Smith, L.M., J.Z. Sander, R.J. Kaiser, P. Hughes, C. Dodd, C.R. Connel, C. Heiner, S.B. Kent, and L.E. Hood. 1986. Fluorescence detection in automated sequence analysis. *Nature.* 321:674–679.

56. Vassar, R., J. Ngai, and R. Axel. 1993. Spatial segregation of odorant receptor expression in the mammalian olfactory epithelium. *Cell.* 74:309–318.

57. Wang, T., P.K. Donahoe, and A.S. Zervos. 1994. Specific interaction of type I receptors of the TGFβ family with the immunophilin FKBP-12. *Science.* 265:674–676.

58. Wang, T., B. Li, P.D. Danielson, P.C. Shah, S. Rockwell, R.J. Lechleider, J. Martin, T. Manganaro, and P.K. Donahoe. 1996. The immunophilin FKBP12 functions as a common inhibitor of the TGFβ family of type I receptors. *Cell.* 86:435–444.